Copy 5
RM L52G07



NACA

# RESEARCH MEMORANDUM

## WIND-TUNNEL INVESTIGATION OF THE LOW-SPEED STATIC AND ROTARY STABILITY DERIVATIVES OF A 0.13-SCALE MODEL OF THE DOUGLAS D-558-II AIRPLANE IN THE LANDING CONFIGURATION

By M. J. Queijo and Evalyn G. Wells

Langley Aeronautical Laboratory
Langley Field, Va.



NATIONAL ADVISORY COMMITTEE FOR AERONAUTICS

WASHINGTON

August 27, 1952

NATIONAL ADVISORY COMMITTEE FOR AERONAUTICS

RESEARCH MEMORANDUM

# WIND-TUNNEL INVESTIGATION OF THE LOW-SPEED STATIC AND ROTARY STABILITY DERIVATIVES OF A 0.13-SCALE MODEL OF THE DOUGLAS D-558-II AIRPLANE IN THE LANDING CONFIGURATION

By M. J. Queijo and Evalyn G. Wells

## SUMMARY

A wind-tunnel investigation has been made to determine the low-speed static and rotary stability derivatives of a 0.13-scale model of the Douglas D-558-II airplane in the landing configuration. The lift coefficient of the model varied linearly with angle of attack up to a maximum lift coefficient of 1.24 which occurred at an angle of attack of 13°. The lift-curve slope was about 0.06 per degree in this range. The model was longitudinally stable in the angle-of-attack range from 0° to 16°, with a static margin of about 16 percent of the wing mean aerodynamic chord over most of this range. The model was approximately neutrally stable near an angle of attack of 11°.

The directional stability of the model decreased slowly with increase in angle of attack up to an angle of attack of about 13°. At higher angles, the stability deteriorated more rapidly. The yawing moment due to rolling velocity was negative throughout the angle-of-attack range, and the magnitude of the tail contribution to this moment near zero angle of attack indicated a stronger sidewash effect for the flapped wing than generally has been obtained for plain wings.

The derivatives associated with yawing flow were nearly constant for angles of attack from 0° to about 13°, but varied considerably at higher angles.

## INTRODUCTION

Various investigations have shown that the dynamic lateral stability characteristics of high-speed aircraft are critically dependent on certain mass and aerodynamic parameters and, hence, that reliable estimates of the dynamic stability of such aircraft can be made only if these parameters are determined accurately. The static derivatives of an airplane can be determined accurately by means of conventional wind-tunnel tests of a model; however, only a few facilities are available for measuring rotary (rolling and yawing) derivatives. The Langley stability tunnel, which is equipped with facilities for simulating rolling and yawing flow, was utilized to make available measured low-speed static and rotary derivatives of a model of the Douglas D-558-II airplane in the landing configuration (slats, flaps, and landing gear extended). The measured low-speed parameters of the same model with slats, flaps, and landing gear retracted are given in reference 1.

## SYMBOLS AND COEFFICIENTS

The data presented herein are in the form of standard NACA coefficients of forces and moments which are referred to the system of stability axes (fig. 1) with the origin at the projection of the quarter-chord point of the wing mean aerodynamic chord on the plane of symmetry. This system of axes is defined as an orthogonal system having the origin at the center of gravity and in which the Z-axis is in the plane of symmetry and perpendicular to the relative wind, the X-axis is in the plane of symmetry and perpendicular to the Z-axis, and the Y-axis is perpendicular to the plane of symmetry. Positive directions of forces, moments, and displacements are shown in figure 1.

$b$ wing span, ft

$c$ local wing chord, parallel to plane of symmetry, ft

$\bar{c}$ mean aerodynamic chord, ft

$p$ rolling angular velocity, radians/sec

$q$ dynamic pressure, $\frac{1}{2}\rho V^2$, lb/sq ft

$r$ yawing angular velocity, radians/sec

$S$ wing area, sq ft

$V$ free-stream velocity, ft/sec

$\alpha$ angle of attack, deg

$\beta$ sideslip angle, radians

$\gamma$ angle of climb, deg

$\psi$ angle of yaw, deg

$\phi$ angle of roll, deg

$\rho$ mass density of air, slugs/cu ft

D drag, lb

L lift, lb

Y side force, lb

M pitching moment, ft-lb

N yawing moment, ft-lb

$l$ rolling moment, ft-lb

$C_D$ drag coefficient, $D/qS$

$C_L$ lift coefficient, $L/qS$

$C_Y$ side-force coefficient, $Y/qS$

$C_m$ pitching-moment coefficient, $M/qS\bar{c}$

$C_n$ yawing-moment coefficient, $N/qSb$

$C_l$ rolling-moment coefficient, $l/qSb$

$$C_{Y_\beta} = \frac{\partial C_Y}{\partial \beta}$$

$$C_{n_\beta} = \frac{\partial C_n}{\partial \beta}$$

$$C_{l_\beta} = \frac{\partial C_l}{\partial \beta}$$

$$C_{Y_p} = \frac{\partial C_Y}{\partial \frac{pb}{2V}}$$

$$C_{n_p} = \frac{\partial C_n}{\partial \frac{pb}{2V}}$$

$$C_{l_p} = \frac{\partial C_l}{\partial \frac{pb}{2V}}$$

$$C_{Y_r} = \frac{\partial C_Y}{\partial \frac{rb}{2V}}$$

$$C_{n_r} = \frac{\partial C_n}{\partial \frac{rb}{2V}}$$

$$C_{l_r} = \frac{\partial C_l}{\partial \frac{rb}{2V}}$$

## APPARATUS, MODEL, AND TESTS

The tests of the present investigation were conducted in the 6-foot-diameter rolling-flow and 6- by 6-foot yawing-flow test sections of the Langley stability tunnel, in which rolling and yawing flow are simulated by curving the air stream about a stationary model (refs. 2 and 3). A single-strut support was used to attach the model to a six-component balance system.

The model used in the investigation was a 0.13-scale model of the Douglas D-558-II airplane and was constructed of laminated mahogany. A drawing of the model is given as figure 2, with details of the flaps and slats given in figure 3. Pertinent geometric characteristics of the model are listed in table I, and a photograph of the model used in the investigation is presented as figure 4.

Tests in straight and rolling flow were made at a dynamic pressure of 39.7 pounds per square foot, which corresponds to a Mach number of 0.17, and a Reynolds number of 1,100,000 based on the wing mean aerodynamic chord. The tests in sideslip and in yawing flow were made at a dynamic pressure of 24.9 pounds per square foot, corresponding to a Mach number of 0.13 and a Reynolds number of 865,000. Tests were made with the complete model and also with the wing-fuselage combination.

## CORRECTIONS

Approximate corrections for jet-boundary effects were applied to the angle of attack by the methods of reference 4 and to the pitching-moment coefficient by the methods of reference 5.

## RESULTS AND DISCUSSION

### Static Longitudinal Characteristics

The lift coefficient of the model in the landing configuration increased linearly with angle of attack up to $\alpha = 13^{\circ}$, and the lift-curve slope $\partial C_L/\partial\alpha$ was about 0.06 per degree (fig. 5). A maximum lift coefficient of 1.24 was attained at $\alpha = 13^{\circ}$, and remained near that value for angles of attack from $13^{\circ}$ to $22^{\circ}$. The model was longitudinally stable (negative $\partial C_m/\partial\alpha$) in the angle-of-attack range from $0^{\circ}$ to about $16^{\circ}$ with a static margin of about $0.16\bar{c}$ over most of the range. The model was approximately neutrally stable near $\alpha = 11^{\circ}$. At angles of attack above about $16^{\circ}$, the pitching-moment coefficient changed erratically with angle of attack.

### Static Lateral Characteristics

The directional instability of the wing-fuselage combination (negative $C_{n_\beta}$) was approximately constant through the angle-of-attack range (fig. 6). Addition of the tail surfaces made the model directionally stable throughout most of the angle-of-attack range; however, the degree of stability generally decreased with increase in angle of attack. The effective-dihedral parameter $C_{l_\beta}$ was approximately the same for the wing-fuselage combination as it was for the complete model, and generally increased negatively with an increase in angle of attack.

### Characteristics in Rolling Flow

The aerodynamic derivatives of the model in simulated roll are shown in figure 7 as curves of $C_{Y_p}$, $C_{n_p}$, and $C_{l_p}$ plotted against angle of attack. Addition of the tail surfaces to the wing-fuselage combination produced a negative increment of $C_{n_p}$. From geometric considerations, such as those of reference 6, a positive increment to $C_{n_p}$ would have been expected near $\alpha = 0^{\circ}$ from addition of the tail surfaces. The negative increment actually obtained probably is caused by changes in flow angularity at the tail plane, associated with wing wake characteristics (ref. 7). It appears that deflection of the flaps has a rather powerful effect on the flow angularity at the tail since, in investigations with models having plain wings, the positive tail contribution to $C_{n_p}$ at $\alpha = 0^{\circ}$, although reduced by wing wake angularity, has not been made negative (for example, see refs. 7, 8, or 9).

## Characteristics in Yawing Flow

The yawing-flow parameters $C_{Y_r}$, $C_{n_r}$, and $C_{l_r}$ are plotted against angle of attack in figure 8. These parameters remained approximately constant for angles of attack up to about 13° for the model with the tail surfaces on or off. At angles of attack greater than 13°, the parameters varied over a rather large range with increase in angle of attack.

## CONCLUSIONS

An investigation was made in the Langley stability tunnel to determine the low-speed static and rotary stability derivatives of a 0.13-scale model of the Douglas D-558-II airplane in the landing configuration. The results of the investigation have led to the following conclusions:

1. The lift coefficient varied linearly with angle of attack up to a maximum lift coefficient of 1.24, which occurred at an angle of attack of 13°. The lift-curve slope was about 0.06 per degree in this range.

2. The model had static longitudinal stability in the angle-of-attack range from 0° to about 16° with a static margin of about 16 percent of the wing mean aerodynamic chord over most of the range. The model was approximately neutrally stable near an angle of attack of 11°.

3. The directional stability of the model decreased slowly with increase in angle of attack up to about 13°. At higher angles of attack, the directional stability generally decreased more rapidly.

4. The yawing moment due to roll $C_{n_p}$ was negative throughout the angle-of-attack range. The magnitude of the tail contribution to $C_{n_p}$ at low angles of attack indicated a stronger sidewash effect in roll for the flapped wing than generally has been obtained for plain wings.

5. The derivatives associated with yawing flow were about constant in the angle-of-attack range from $0^{\circ}$ to $13^{\circ}$, and varied considerably with angle of attack above $13^{\circ}$.

Langley Aeronautical Laboratory
National Advisory Committee for Aeronautics
Langley Field, Va.

REFERENCES

1. Queijo, M. J., and Goodman, Alex: Calculations of the Dynamic Lateral Stability Characteristics of the Douglas D-558-II Airplane in High-Speed Flight for Various Wing Loadings and Altitudes. NACA RM L50H16a, 1950.

2. MacLachlan, Robert, and Letko, William: Correlation of Two Experimental Methods of Determining the Rolling Characteristics of Unswept Wings. NACA TN 1309, 1947.

3. Bird, John D., Jaquet, Byron M., and Cowan, John W.: Effect of Fuselage and Tail Surfaces on Low-Speed Yawing Characteristics of a Swept-Wing Model As Determined in Curved-Flow Test Section of Langley Stability Tunnel. NACA TN 2483, 1951. (Supersedes NACA RM L8G13.)

4. Silverstein, Abe, and White, James A.: Wind-Tunnel Interference With Particular Reference to Off-Center Positions of the Wing and to the Downwash at the Tail. NACA Rep. 547, 1936.

5. Gillis, Clarence L., Polhamus, Edward C., and Grey, Joseph L., Jr.: Charts for Determining Jet-Boundary Corrections for Complete Models in 7- by 10-Foot Closed Rectangular Wind Tunnels. NACA ARR L5G31, 1945.

6. Bamber, Millard J.: Effect of Some Present-Day Airplane Design Trends on Requirements for Lateral Stability. NACA TN 814, 1941.

7. Michael, William H., Jr.: Analysis of the Effects of Wing Interference on the Tail Contribution to the Rolling Derivatives. NACA TN 2332, 1951.

8. Letko, William, and Riley, Donald R.: Effect of an Unswept Wing on the Contribution of Unswept-Tail Configurations to the Low-Speed Static- and Rolling-Stability Derivatives of a Midwing Airplane Model. NACA TN 2175, 1950.

9. Wolhart, Walter D.: Influence of Wing and Fuselage on the Vertical-Tail Contribution to the Low-Speed Rolling Derivatives of Midwing Airplane Models With 45° Sweptback Surfaces. NACA TN 2587, 1951.

TABLE I.- DIMENSIONS AND CHARACTERISTICS OF MODEL

| | |
|---|---|
| Wing: | |
| Root airfoil section (normal to 0.33-chord line) | NACA 63-010 |
| Tip airfoil section (normal to 0.33-chord line) | NACA 63-012 |
| Total area, sq in. | 428 |
| Span, in. | 38.84 |
| Mean aerodynamic chord, in. | 11.30 |
| Root chord (parallel to plane of symmetry), in. | 14.10 |
| Tip chord (parallel to plane of symmetry), in. | 7.95 |
| Taper ratio | 0.565 |
| Aspect ratio | 3.57 |
| Sweep at 0.33-chord line, deg | 35.0 |
| Incidence, deg | 3.0 |
| Dihedral, deg | -3.0 |
| Total flap area, sq in. | 31.50 |
| Horizontal Tail: | |
| Airfoil section (normal to 0.35-chord line) | NACA 63-010 |
| Total area, sq in. | 97.10 |
| Span, in. | 18.66 |
| Mean aerodynamic chord, in. | 5.42 |
| Root chord (parallel to plane of symmetry), in. | 6.97 |
| Tip chord (parallel to plane of symmetry), in. | 3.48 |
| Taper ratio | 0.50 |
| Aspect ratio | 3.59 |
| Sweep at 0.35-chord line, deg | 40.0 |
| Incidence (from fuselage center line), deg | 0 |
| Tail length (from $\bar{c}/4$ of wing to $\bar{c}/4$ of tail), in. | 30.58 |
| Tail height (from fuselage center line), in. | 6.60 |
| Vertical Tail: | |
| Airfoil section (normal to 0.45-chord line) | NACA 63-010 |
| Root chord (parallel to fuselage center line), in. | 18.90 |
| Height, from fuselage center line, in. | 12.68 |
| Sweep at 0.45-chord line, deg | 49.0 |
| Fuselage: | |
| Length, in. | 65.52 |
| Maximum diameter, in. | 7.80 |
| Fineness ratio | 8.40 |

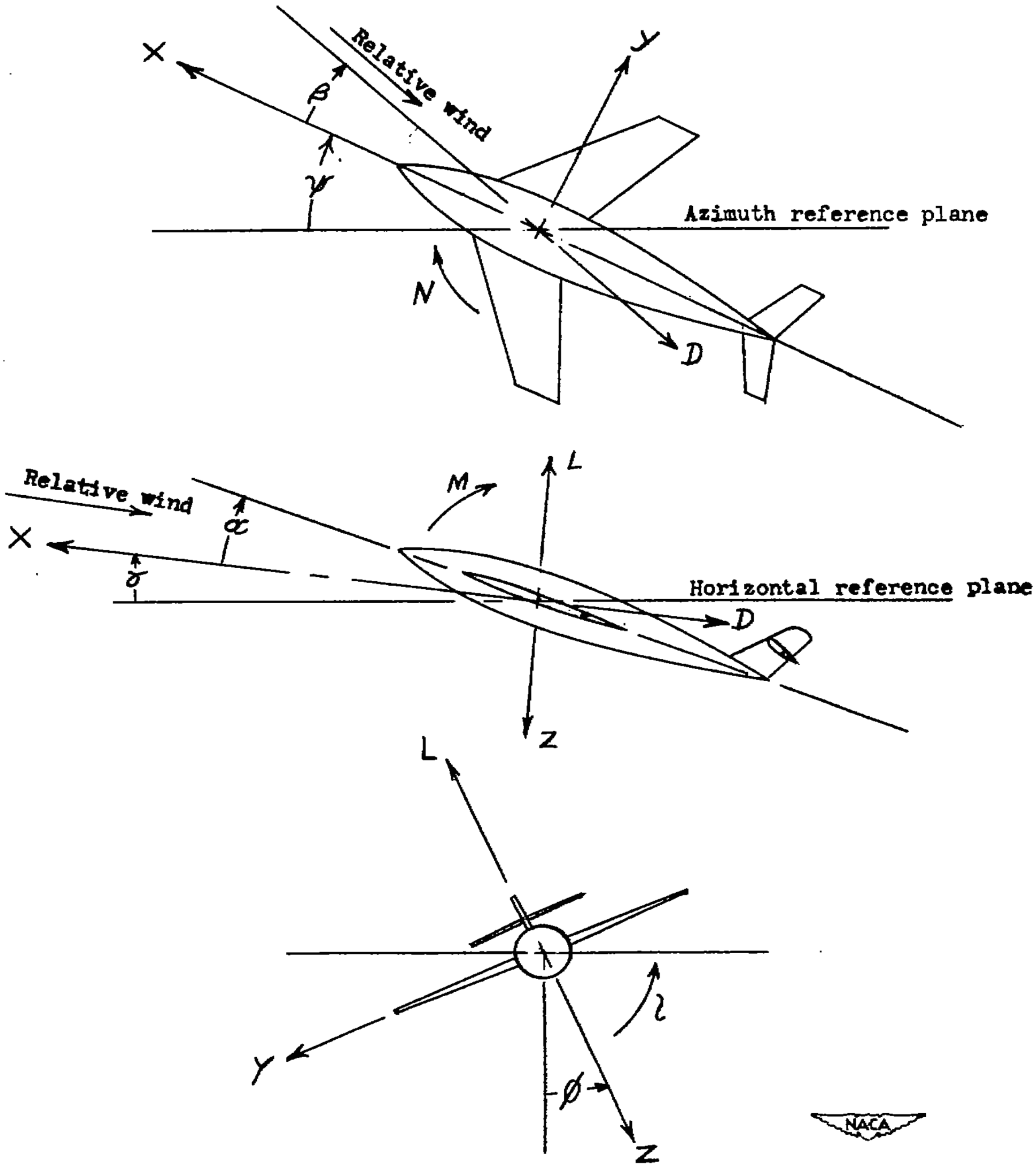


Figure 1.- System of stability axes. Arrows indicate positive direction of forces, moments, and displacements.

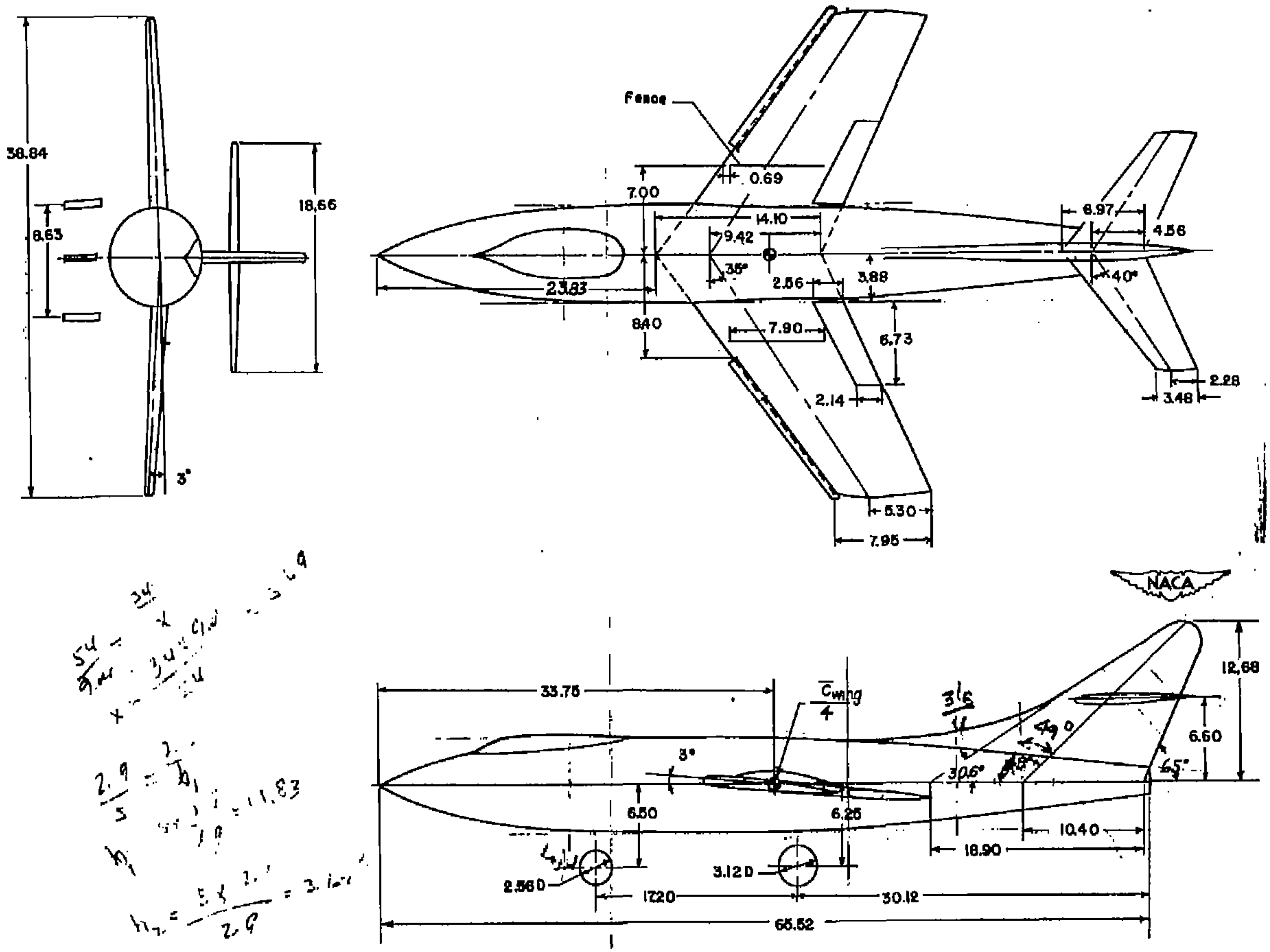


Figure 2.- Model used in the investigation. All dimensions given in inches.

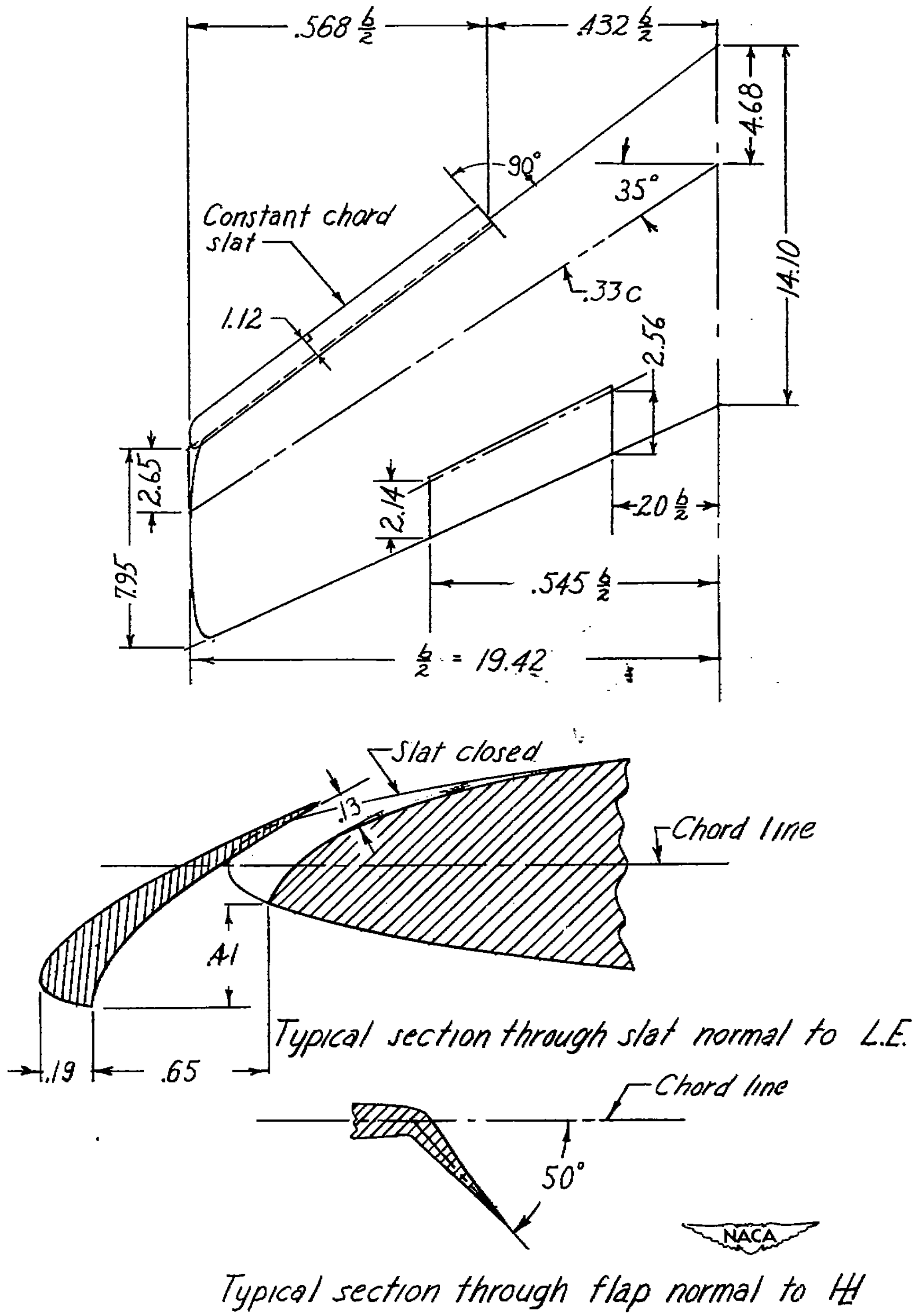


Figure 3.- Details of slats and plain flaps. All dimensions given in inches.

[redacted]

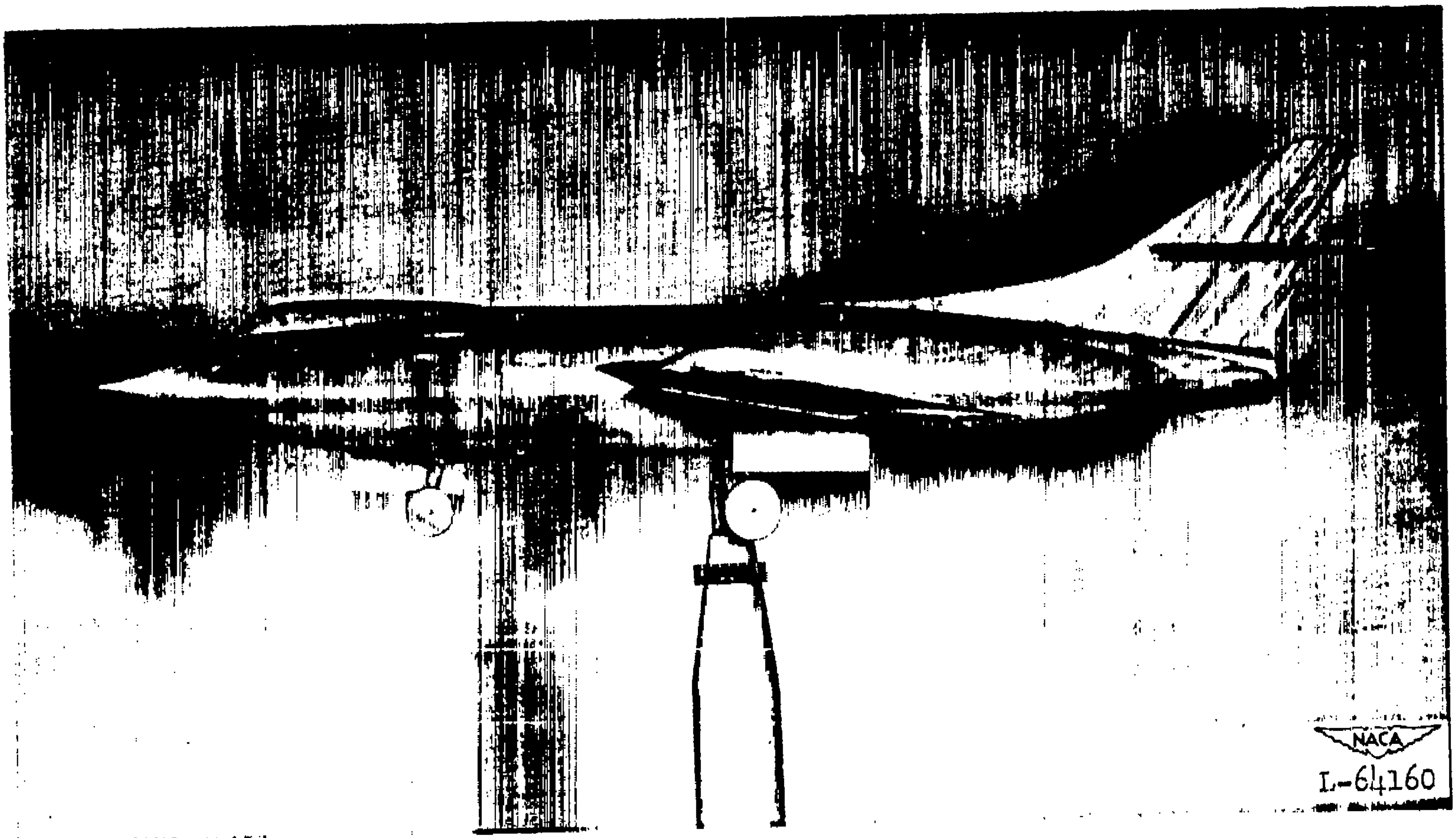


Figure 4.- Model used in tests.

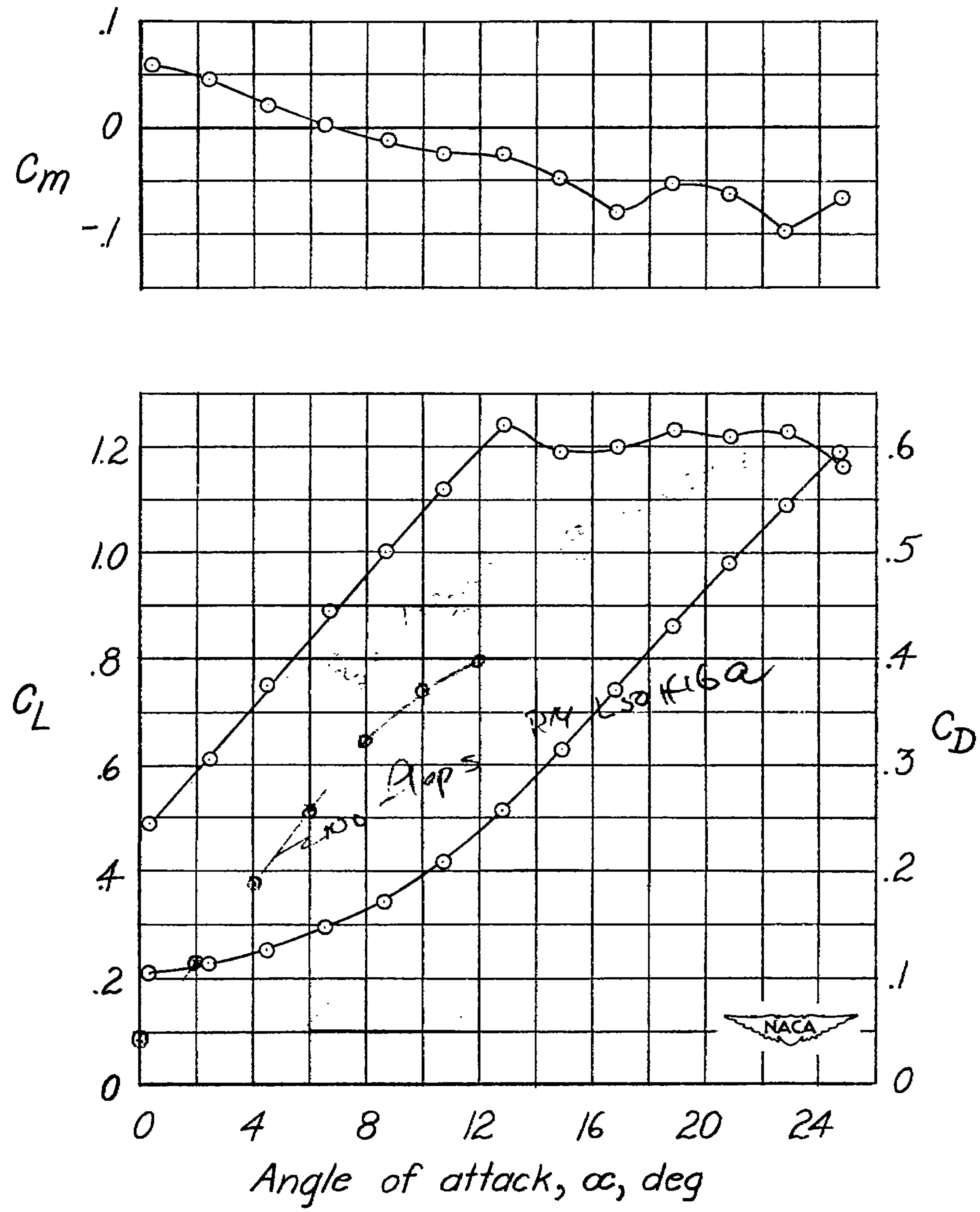


Figure 5.- Variation of $C_L$, $C_D$, and $C_m$ with $\alpha$ for a 0.13-scale model of the D-558-II airplane in the landing configuration. Mach number, 0.17; Reynolds number, 1,100,000.

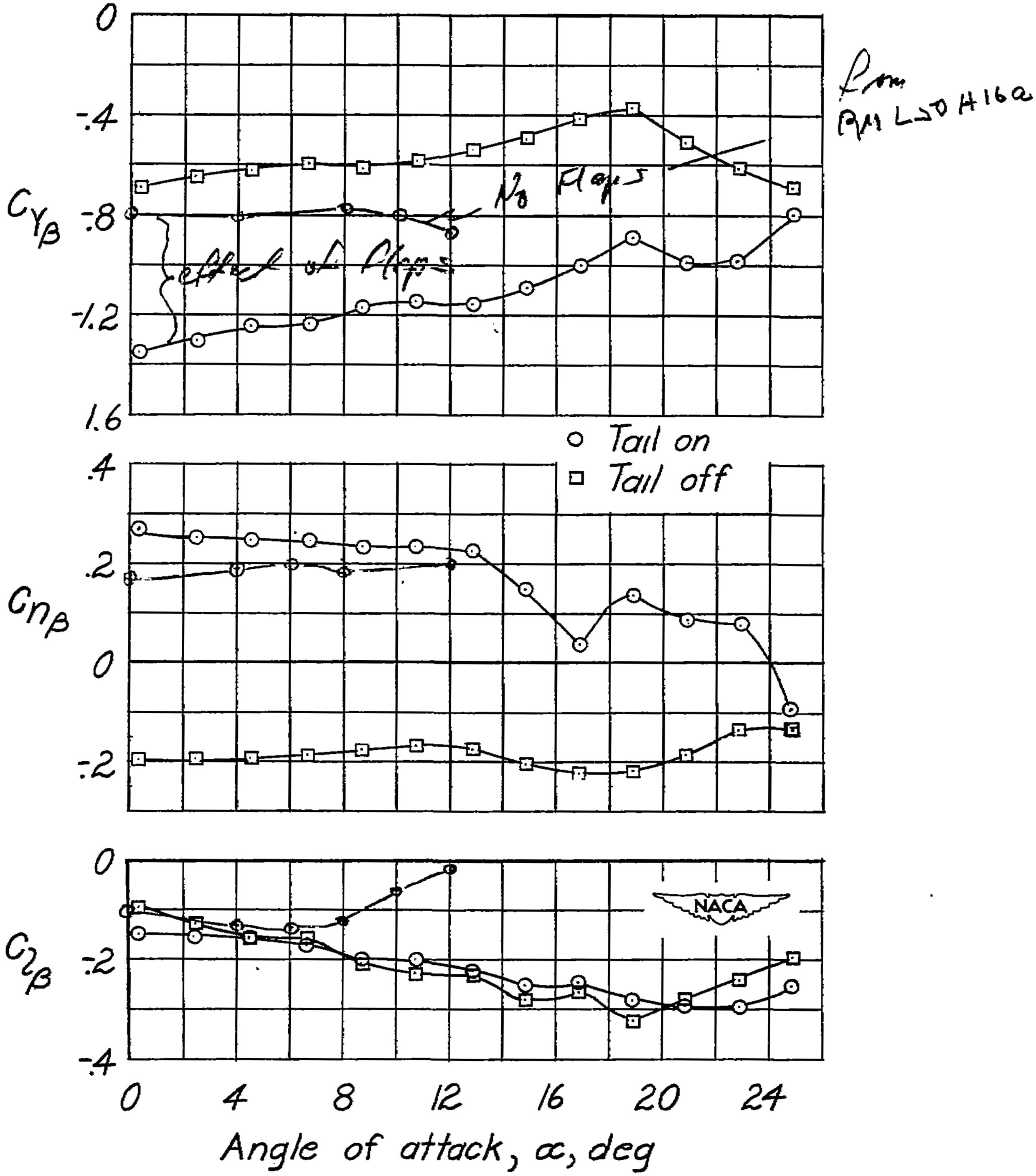


Figure 6.- Variation of $C_{Y_\beta}$, $C_{n_\beta}$, and $C_{l_\beta}$ with $\alpha$ for a 0.13-scale model of the D-558-II airplane in the landing configuration. Mach number, 0.17; Reynolds number, 1,100,000.

[redacted]

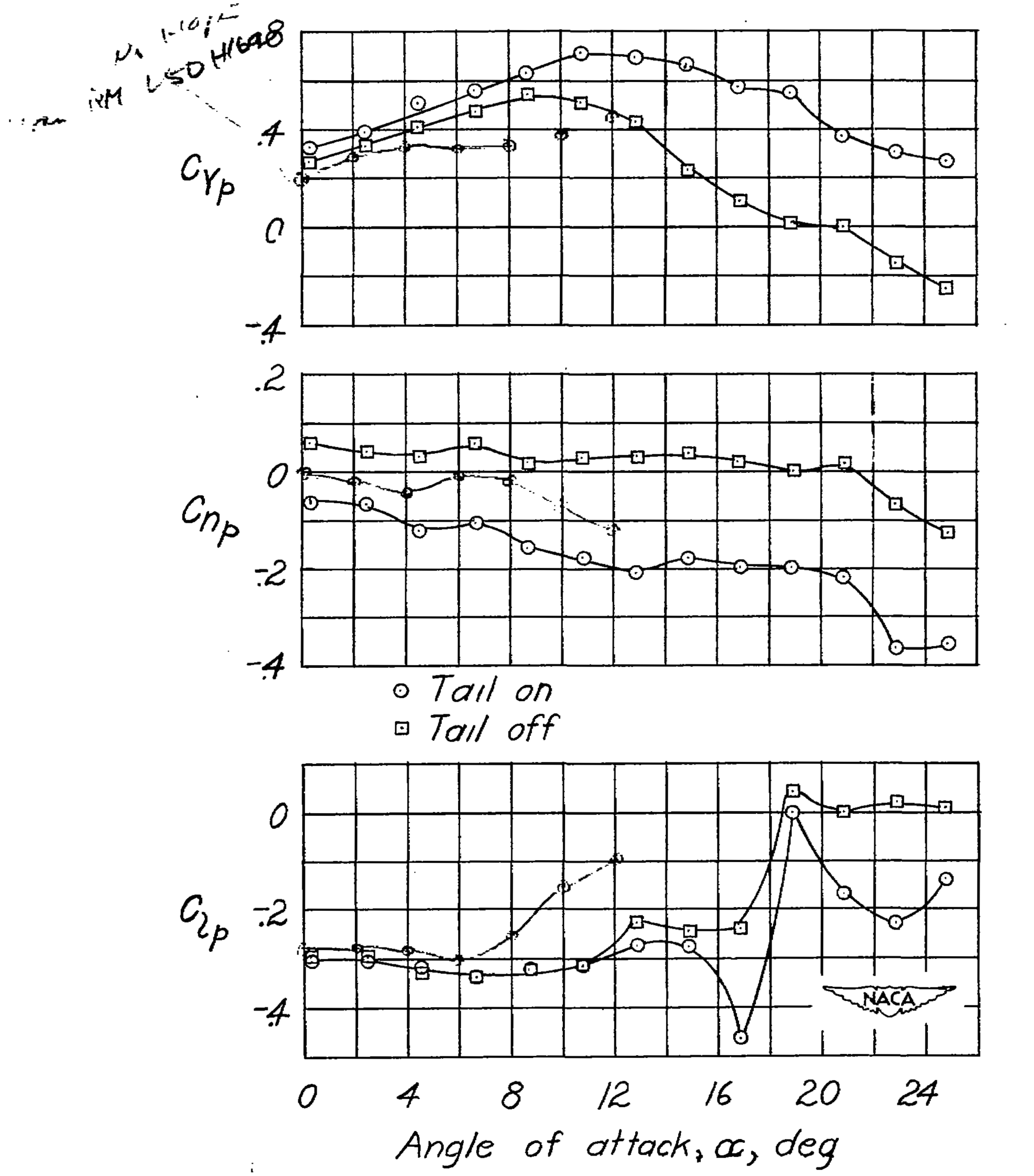


Figure 7.- Variation of $C_{Y_p}$, $C_{n_p}$, and $C_{l_p}$ with $\alpha$ for a 0.13-scale model of the D-558-II airplane in the landing configuration. Mach number, 0.17; Reynolds number, 1,100,000.

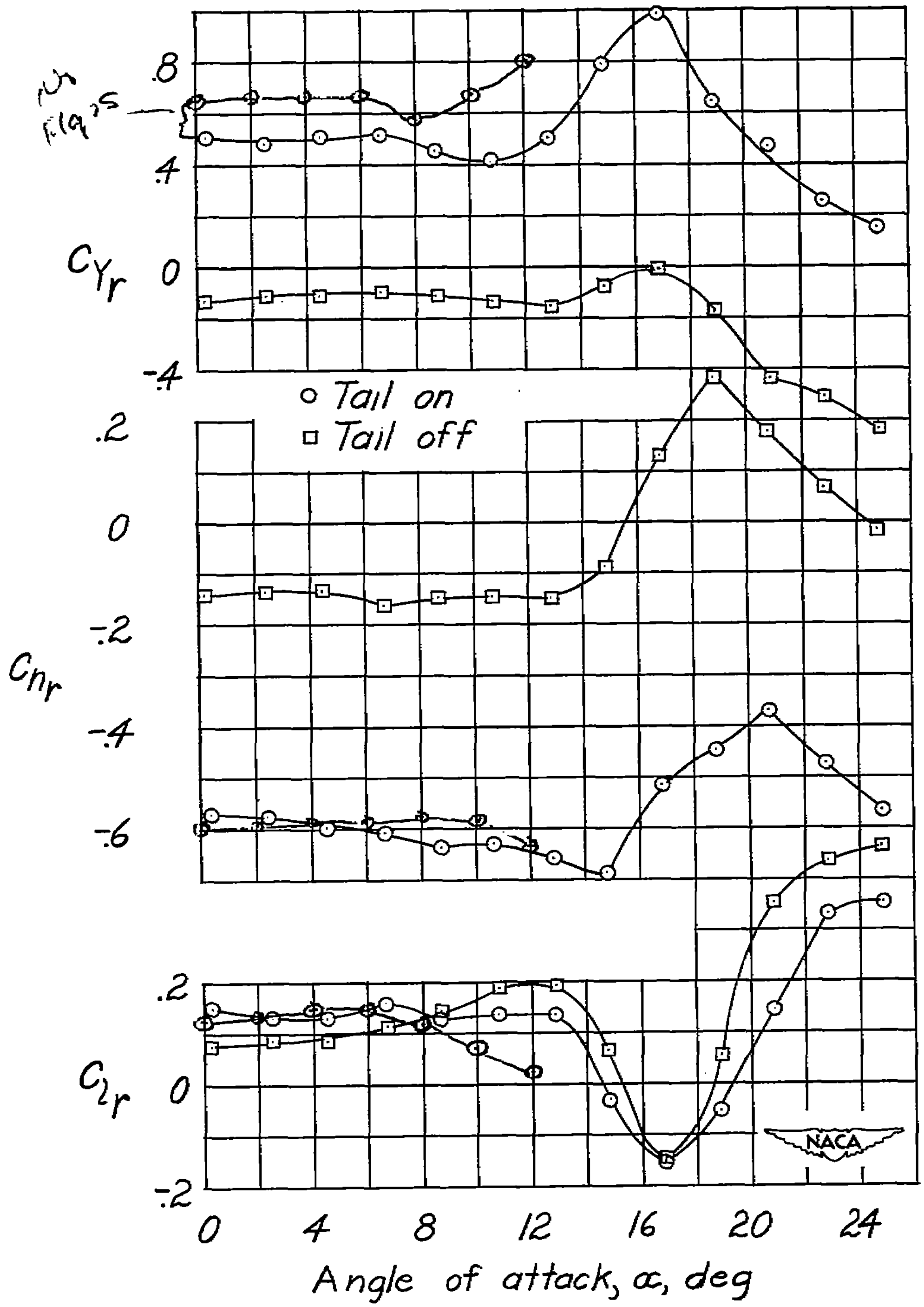


Figure 8.- Variation of $C_{Y_r}$, $C_{n_r}$, and $C_{l_r}$ with $\alpha$ for a 0.13-scale model of the D-558-II airplane in the landing configuration. Mach number, 0.13; Reynolds number, 865,000.

[redacted]

SECURITY INFORMATION



[redacted]